

THE ACCURACY OF LINEARIZED ELASTIC PARAMETER ESTIMATION

B. URSIN and E. TJÅLAND

University of Trondheim, Div. of Petroleum Engineering and Applied Geophysics, N-7034 Trondheim, Norway.

(Received April 5, 1993; revised version accepted September 1, 1993)

ABSTRACT

Ursin, B. and Tjøland, E., 1993. The accuracy of linearized elastic parameter estimation. *Journal of Seismic Exploration*, 2: 349-363.

Angle-dependent reflection coefficients contain information about elastic parameters in the subsurface, providing the basis for amplitude versus offset (AVO) analysis. Parameter estimates have been derived using angle-dependent and offset-dependent linearized PP reflection coefficients with two different parameterizations. Statistical properties of parameter estimates obtained from AVO analysis are investigated using model parameter confidence regions. The relative change in acoustic impedance is the best-determined elastic parameter. The normalized change in Poisson's ratio and the normalized change in shear modulus are the second best determined parameters for the two parameterizations respectively. The normalized change in the shear modulus is better determined than the normalized change in the Poisson's ratio. The parameterization using shear modulus therefore seems to give better results than using Poisson's ratio. The worst-determined parameter is the relative change in P-wave velocity.

KEY WORDS: AVO, reflection coefficients, parameter estimation, sensitivity analysis, uncertainty analysis, inversion.

INTRODUCTION

Seismic amplitude variation with offset (AVO) caused by angle-dependent reflection coefficients can, in principle, be used to estimate elastic parameters. AVO analysis has been used successfully to predict the presence of hydrocarbons, but in some cases it has failed (Allen et al., 1993). To understand why this happens, a natural approach is to look at the information content of the angle-dependent reflection coefficients.

Linearized AVO inversion based on the 'small contrast approximation' Aki and Richards, 1980; Shuey, 1985) relate the reflection coefficients linearly to the relative change in elastic parameters. Linearized AVO inversion can produce seismic sections having amplitudes proportional to parameter changes (Smith and Gidlow, 1987). Swan (1990) performed a covariance analysis of the information content of the linearized reflection coefficients, and de Nicolao et al. (1993) performed a complete eigenvector analysis of a different parameterization. In both cases the data were given as a function of angle.

We have investigated the information content of linearized PP reflection coefficients as a function of angle in addition to the related linearized PP reflection coefficients as a function of offset, using two different parameterizations. The transformation from angle to offset has been performed using reflectivity polynomials. Using this new set of approximations for the reflection coefficient, we have found explicit expressions for the inverse covariance matrices for various model parameters. These inverse covariance matrices correspond to confidence regions in the model space. From the eigenvalues and eigenvectors of the normalized inverse covariance matrices, the best- and worst-determined parameter combinations are found. We have investigated different parameterizations than Swan (1990) and de Nicolao et al. (1993), introducing one which includes the normalized shear modulus (which is independent of the P- to S-wave velocity ratio), and another which involves the normalized contrast in the Poisson's ratio. The latter parameterization depends on the P- to S-wave velocity ratio, and is therefore model dependent. To solve this problem we have calculated a distribution of eigenvalues and eigenvectors for a range of P- to S-wave velocity ratios.

MODEL PARAMETER ESTIMATION IN ANGULAR COORDINATES

Estimation of the shear modulus

The PP reflection coefficient may be approximated by assuming small contrasts in the elastic parameters (Aki and Richards, 1980). Different parameterizations result in slightly different approximations. An approximation (Thomsen, 1990; Ursin and Tjåland, 1992) which seems simple to interpret is:

$$R \approx R_1 = \frac{1}{2}(\Delta Z_p/Z_p) - 2\sin^2\theta(\Delta\mu/M) + \frac{1}{2}\tan^2\theta(\Delta\alpha/\alpha), \quad (1)$$

where Z_p is the average of the P-wave acoustic impedance across the interface, μ the average shear-modulus, $M = K + 4\mu/3$ the average plane-wave modulus, K the average bulk modulus, α the average P-wave velocity, θ the average of the angle of incidence and the angle of transmission of the P-wave, and ΔZ_p , $\Delta\mu$ and $\Delta\alpha$ the changes in Z_p , μ and α across the interface.

Assuming the PP reflection coefficient $R(\theta)$ to be known for K discrete values of θ , the data are given by $\mathbf{d}_1 \approx \mathbf{A}\mathbf{m}_1$, where the rows of the matrix \mathbf{A} are

$$(\frac{1}{2}, -2\sin^2\theta_k, \frac{1}{2}\tan^2\theta_k), \quad k = 0, K-1.$$

The model parameter vector \mathbf{m}_1 , representing relative changes in the elastic parameters across the interface, is given by $\mathbf{m}_1 = (\Delta Z_p/Z_p, \Delta\mu/M, \Delta\alpha/\alpha)^T$. The least-squares estimate of the model parameters is now

$$\hat{\mathbf{m}}_1 = (\mathbf{A}^T\mathbf{A})^{-1}\mathbf{A}^T\mathbf{d}_1 \quad (2)$$

with \mathbf{A} defined as above.

Estimation of the Poisson's ratio

An alternative linearized expression for the PP reflection coefficient was proposed by Shuey (1985). Equation (14) in Shuey's paper can be rearranged as follows:

$$R \approx R_2 = [\frac{1}{2} - 2(\beta/\alpha)^2\sin^2\theta](\Delta Z_p/Z_p) + \sin^2\theta[\Delta v/(1-v)^2] + [\frac{1}{2}\tan^2\theta - 2(\beta/\alpha)^2\sin^2\theta](\Delta\alpha/\alpha), \quad (3)$$

where the average Poisson's ratio at the interface is v , and the change in the Poisson's ratio is Δv . The reflection amplitude data can now be approximated by $\mathbf{d}_1 \approx \mathbf{B}\mathbf{m}_2$, where the rows of the matrix \mathbf{B} are

$$[\frac{1}{2} - 2(\beta/\alpha)^2\sin^2\theta_k, \sin^2\theta_k, \frac{1}{2}\tan^2\theta_k - 2(\beta/\alpha)^2\sin^2\theta_k], \quad k = 0, K-1,$$

and the new model parameter vector $\mathbf{m}_2 = [\Delta Z_p/Z_p, \Delta v/(1-v)^2, \Delta\alpha/\alpha]^T$. The least squares estimate of \mathbf{m}_2 is given by

$$\hat{\mathbf{m}}_2 = (\mathbf{B}^T\mathbf{B})^{-1}\mathbf{B}^T\mathbf{d}_1. \quad (4)$$

MODEL PARAMETER ESTIMATION IN OFFSET COORDINATES

Estimation of the shear modulus

Model parameters can be estimated as a function of offset directly from seismic data using reflectivity polynomials (Denham et al., 1985; Ursin and Dahl, 1990; Ursin and Ekren, 1992). The coefficients of the reflectivity polynomial are related to the relative changes in elastic properties (the model parameter vector) by a linear transformation (Balogh et al., 1986).

A small offset approximation of (1) gives

$$R \approx R_3 = \frac{1}{2}(\Delta Z_p/Z_p) + [\frac{1}{2}(\Delta\alpha/\alpha) - 2(\Delta\mu/M)](\alpha p)^2 + \frac{1}{2}(\Delta\alpha/\alpha)(\alpha p)^4 \\ = a_0 + a_1(\alpha p)^2 + a_2(\alpha p)^4, \quad (5)$$

where $\alpha p = \sin\theta$, and p is slowness.

The model parameter vector \mathbf{m}_1 is related to the coefficient vector $\mathbf{a} = (a_0, a_1, a_2)^T$ in (5) by

$$\mathbf{m}_1 = \begin{bmatrix} 2 & 0 & 0 \\ 0 & -1/2 & 1/2 \\ 0 & 0 & 2 \end{bmatrix} \mathbf{a}. \quad (6)$$

Seismic amplitudes for a constant time in an NMO-corrected CMP gather can be expressed as a reflectivity polynomial in offset coordinates $\mathbf{d}_2 \approx \mathbf{Y}\mathbf{r}$, where the rows of the offset matrix \mathbf{Y} are

$$(1, y_k^2, y_k^4), \quad k = 0, K-1,$$

and the coefficient vector is $\mathbf{r} = (r_0, r_1, r_2)^T$. Above, y_k are the offset values and N is the number of traces in the CMP gather. The least-squares estimate of the coefficients in the reflectivity polynomial is

$$\hat{\mathbf{r}} = (\mathbf{Y}^T\mathbf{Y})^{-1}\mathbf{Y}^T\mathbf{d}_2. \quad (7)$$

The coefficient vector, \mathbf{a} , of the slowness polynomial in equation (5) can be obtained from the coefficient vector, \mathbf{r} , of the offset polynomial using a standard technique (Taner and Koehler, 1969; Ursin and Dahl, 1992),

$$\mathbf{a} = \begin{bmatrix} 1 & 0 & 0 \\ 0 & g & 0 \\ 0 & h & g^2 \end{bmatrix} \hat{\mathbf{r}}. \quad (8)$$

where $g = b_1^2/\alpha^2$ and $h = b_1b_2/\alpha^4$. The velocity moments b_j are defined as

$$b_j = \int_{\text{PP}} \alpha(z)^{j-1} dz = 2 \int_0^d \alpha(z)^{j-1} dz \quad (9)$$

for a primary PP reflected wave (z denotes vertical depth, positive downwards,

and d is reflector depth). Note that for a constant velocity layer, α is constant and $g = h = 4d^2$.

Combining (6) and (8) gives the new estimate of \mathbf{m}_1 (Balogh et al., 1986)

$$\hat{\mathbf{m}}_1 = \mathbf{G}\hat{\mathbf{r}} = \begin{bmatrix} 2 & 0 & 0 \\ 0 & (h-g)/2 & g^2/2 \\ 0 & 2h & 2g^2 \end{bmatrix} \hat{\mathbf{r}}. \quad (10)$$

Estimation of the Poisson's ratio

The small offset approximation of (3) is given by

$$R \approx R_4 = \frac{1}{2}(\Delta Z_p/Z_p) \\ + [\Delta v/(1-v)^2 - 2(\beta/\alpha)^2\{(\Delta Z_p/Z_p) + (\Delta\alpha/\alpha)\} + \frac{1}{2}(\Delta\alpha/\alpha)](\alpha p)^2 \\ + \frac{1}{2}(\Delta\alpha/\alpha)(\alpha p)^4, \quad (11)$$

and is valid for small reflection angles.

Combining the reflectivity polynomial and the coefficients of (11) in the same way as before gives a new estimate of \mathbf{m}_2 :

$$\hat{\mathbf{m}}_2 = \mathbf{H}\hat{\mathbf{r}} = \begin{bmatrix} 2 & 0 & 0 \\ 4(\beta/\alpha)^2 & 4h(\beta/\alpha)^2 + g - h & g^2[4(\beta/\alpha)^2 - 1] \\ 0 & 2h & 2g^2 \end{bmatrix} \hat{\mathbf{r}}. \quad (12)$$

COVARIANCE MATRICES OF THE ESTIMATED PARAMETERS

The covariance matrix of the estimated model parameters above depends on the distribution of data errors. The data errors are assumed to be independent and identically Gaussian distributed with zero mean and variance σ_1^2 for the angle-dependent data vector \mathbf{d}_1 , and σ_2^2 for the offset-dependent data vector \mathbf{d}_2 . The covariance matrix of the estimated model parameter vector $\hat{\mathbf{m}}_1$ in equation (2) is then

$$\text{Cov}\{\hat{\mathbf{m}}_1\} = \sigma_1^2(\mathbf{A}^T\mathbf{A})^{-1} \approx (\sigma_1^2/\mathbf{K})\mathbf{P}^{-1}, \quad (13)$$

where K is the number of data points. The matrix \mathbf{P} is derived by replacing the sums in the matrix $\mathbf{A}^T \mathbf{A}$ by integrals using the assumptions $\theta_0 = 0$ and equidistant sampling, $\Delta\theta$. The elements $(\mathbf{A}^T \mathbf{A})_{i,j}$ can then be approximated by analytical formulas derived as, for example:

$$\begin{aligned}
 (\mathbf{A}^T \mathbf{A})_{12} &= - \sum_{k=0}^{K-1} \sin^2 \theta_k \approx -K/\theta_k \int_{\theta=0}^{\theta} \sin^2 \theta d\theta \\
 &= - (K/4\theta_k) (2\theta_k - \sin 2\theta_k) = K\mathbf{P}_{12} \quad ,
 \end{aligned}$$

where $\theta_k = K\Delta\theta$ represents the incident angle corresponding to maximum offset.

The covariance matrix of $\hat{\mathbf{m}}_2$ in equation (4) is

$$\text{Cov}\{\hat{\mathbf{m}}_2\} = \sigma_1^2 (\mathbf{B}^T \mathbf{B})^{-1} \approx (\sigma_1^2 / K) \mathbf{Q}^{-1} \quad , \quad (14)$$

where the symmetric matrix \mathbf{Q} is derived similarly to the matrix \mathbf{P} .

The covariance matrix of $\hat{\mathbf{r}}$ in equation (7) is given as

$$\text{Cov}\{\hat{\mathbf{r}}\} = \sigma_2^2 (\mathbf{Y}^T \mathbf{Y})^{-1} \approx (\sigma_2^2 / N) \mathbf{R}^{-1} \quad , \quad (15)$$

where N is the number of traces. The symmetric matrix \mathbf{R} is derived similarly to the matrix \mathbf{P} , except for using offset y instead of angle θ .

The covariance matrices of $\hat{\mathbf{m}}_1$ and $\hat{\mathbf{m}}_2$ in equations (10) and (12) are computed from the covariance of the vector $\hat{\mathbf{r}}$ using the transformation matrices \mathbf{G} and \mathbf{H} , respectively, which give

$$\text{Cov}\{\hat{\mathbf{m}}_1\} \approx (\sigma_2^2 / N) \mathbf{G} \mathbf{R}^{-1} \mathbf{G}^T \quad , \quad (16)$$

$$\text{Cov}\{\hat{\mathbf{m}}_2\} \approx (\sigma_2^2 / N) \mathbf{H} \mathbf{R}^{-1} \mathbf{H}^T \quad . \quad (17)$$

CONFIDENCE REGIONS

Least-squares parameter estimation for a linear model is performed by minimizing the sum of the squared errors between the measured and the modeled data

$$\Phi = \|\mathbf{d} - \mathbf{F}\mathbf{m}\|^2 = (\mathbf{d} - \mathbf{F}\mathbf{m})^T (\mathbf{d} - \mathbf{F}\mathbf{m}) \quad . \quad (18)$$

The minimum error is found for the parameter estimate

$$\hat{\mathbf{m}} = (\mathbf{F}^T \mathbf{F})^{-1} \mathbf{F}^T \mathbf{d} \quad , \quad (19)$$

and then

$$\Phi_{\min} = \|\mathbf{d}\|^2 - \hat{\mathbf{m}}^T \mathbf{F}^T \mathbf{F} \hat{\mathbf{m}} \quad . \quad (20)$$

For a perturbation in the model parameter $\mathbf{m} = \hat{\mathbf{m}} + \Delta\mathbf{m}$ we have

$$\Phi = \Phi_{\min} + \Delta\mathbf{m}^T \mathbf{F}^T \mathbf{F} \Delta\mathbf{m} \quad , \quad (21)$$

which can be verified directly.

Assuming the data errors to be independent and identically normally distributed with zero mean and variance σ^2 , the covariance matrix of the estimated model parameters is given by

$$\text{Cov}\{\hat{\mathbf{m}}\} = \sigma^2 (\mathbf{F}^T \mathbf{F})^{-1} \quad . \quad (22)$$

A confidence region is then given by

$$\Delta\mathbf{m}^T [\text{Cov}\{\hat{\mathbf{m}}\}]^{-1} \Delta\mathbf{m} \leq \chi_K^2 \quad , \quad (23)$$

where χ_K^2 is the chi-square distribution with $K = N - M$ degrees of freedom (N is the number of data points and M is the number of fitted model parameters).

Combining equations (22) and (23) gives the confidence region

$$\Delta\mathbf{m}^T \mathbf{F}^T \mathbf{F} \Delta\mathbf{m} \leq \sigma^2 \chi_K^2 \quad . \quad (24)$$

We now see that a perturbation of the estimated model parameters around the optimal values gives an increase in the error function: $\Delta\Phi = \Phi - \Phi_{\min}$, corresponding to an M -dimensional confidence region around $\hat{\mathbf{m}}$. The confidence regions are ellipsoids given by the quadratic form in equation (24).

In the following we are focusing on the sensitivity of the model parameters by calculating the length and directions of the principal axes of the confidence ellipsoids. This can be accomplished by performing an eigenvalue analysis of $[\text{Cov}\{\hat{\mathbf{m}}\}]^{-1}$. The square roots of the eigenvalues are inversely proportional to the length of the major axes of the ellipsoid, and the corresponding eigenvectors point in the direction of the major axes. Calculation of confidence regions of $\hat{\mathbf{m}}_1$ will serve as an example for the technique used. Inserting (13) into (23) gives the confidence region

$$\Delta\mathbf{m}_1^T \mathbf{P} \Delta\mathbf{m}_1 = (\sigma_1^2 / K) \chi_K^2 \quad . \quad (25)$$

The symmetric matrix \mathbf{P} can be decomposed as

$$\mathbf{P} = \mathbf{U} \mathbf{S} \mathbf{U}^T \quad , \quad (26)$$

where

$$\mathbf{S} = \text{diag}\{\lambda_1, \lambda_2, \lambda_3\} \quad (27)$$

contains the non-negative eigenvalues (λ_i) of \mathbf{P} , and where \mathbf{U} contains the normalized eigenvectors of \mathbf{P} .

The eigenvalues and the eigenvectors of the matrix \mathbf{P} are related to the axes of the normalized ellipsoid

$$\Delta \mathbf{m}_1^T \mathbf{P} \Delta \mathbf{m}_1 = 1 \quad (28)$$

in the following way: the lengths of the principal axes of the ellipsoid are $\lambda_i^{-1/2}$ and the eigenvectors are unit vectors pointing in the direction of the axes.

Table 1 shows the various model estimates and the matrices used to calculate the confidence regions.

Table 1. The various model estimates and the respective inverse normalized covariance matrices used to compute confidence regions.

Data	Model estimate	Inverse normalized covariance matrix
$d_1(\theta)$	$\hat{\mathbf{m}}_1 = [\Delta Z_p/Z_p, \Delta\mu/M, \Delta\alpha/\alpha]^T$ $\hat{\mathbf{m}}_2 = [\Delta Z_p/Z_p, \Delta v/(1-v)^2, \Delta\alpha/\alpha]^T$	\mathbf{P} \mathbf{Q}
$d_2(\gamma)$	$\hat{\mathbf{r}} = (r_0, r_1, r_2)^T$ $\hat{\mathbf{m}}_1 = [\Delta Z_p/Z_p, \Delta\mu/M, \Delta\alpha/\alpha]^T$ $\hat{\mathbf{m}}_2 = [\Delta Z_p/Z_p, \Delta v/(1-v)^2, \Delta\alpha/\alpha]^T$	\mathbf{R} $\mathbf{G}^{-1} \mathbf{R} \mathbf{G}^{-1}$ $\mathbf{H}^{-1} \mathbf{R} \mathbf{H}^{-1}$

NUMERICAL RESULTS

When the data are given as a function of reflection angle, the model parameter estimates depend on the maximum reflection angle, θ_k . When the data are given as a function of offset, the estimates depend on the maximum offset Y_N and the velocity moments b_1 and b_2 defined in equation (9). In order

to simplify the analysis, we have considered a single homogeneous layer of thickness $d = 0.5$ km. This corresponds to $g = h = 1$ in equations (10) and (12). Ellipsoidal confidence regions of the estimated parameters can then be computed as a function of θ_k or Y_N . Each confidence region can be described by three eigenvalues and the corresponding eigenvectors, normalized to unit length. For the estimates $\hat{\mathbf{m}}_2$ and $\hat{\mathbf{m}}_1$, the confidence regions also depend on the given model via the specified α/β -ratio. The computations were therefore performed for a range of α/β -values, gathering the results into histograms. The eigenvalues were first sorted into three data arrays representing the largest, medium and smallest eigenvalues. Each of these arrays was sorted into bins of width 0.02 in a log scale ($0.5 \log \lambda_i$). The numbers of values in each bin were divided by the total number of models, giving a relative frequency distribution of the eigenvalues. A similar procedure was applied to the normalized eigenvectors. For each eigenvalue the components of the eigenvectors were put into bins of width 0.01. This produced three histograms for each eigenvalue. The range of α/β -ratios was chosen so that the Poisson's ratio is positive, $\alpha/\beta > \sqrt{2}$. In the figures eigenvalues and eigenvectors for the confidence regions of $\hat{\mathbf{m}}_2$ and $\hat{\mathbf{m}}_1$ are shown as shaded areas representing a distribution of α/β -ratios for $\alpha/\beta = 1.5$ to 5.0 with increments of 0.01. The legend for the shaded areas is shown to the right of Fig. 3.

Fig. 1 shows the eigenvalues of the matrix \mathbf{P} associated with the parameter estimate $\hat{\mathbf{m}}_1$ as a function of maximum angle θ_k . The plotting scale, $0.5 \log \lambda_i$, represents the half-axes of the confidence ellipsoid in a log scale. The minimum values of θ_k have been chosen larger than zero to avoid zero eigenvalues. For small values of θ_k the medium and smallest eigenvalues approach zero, or minus infinity in the log scale. This is consistent with the fact that only relative change in the P-wave acoustic impedance can be estimated from zero-offset data. It can be concluded that one parameter is well determined, while the other two are poorly determined.

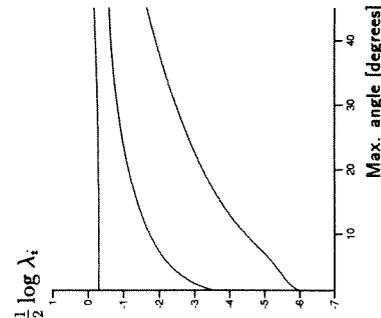


Fig. 1. Eigenvalues of the matrix \mathbf{P} .

Fig. 2 shows the components of the eigenvectors of the matrix **P**. The left, middle and right figures show the components of the eigenvectors corresponding to the largest, medium and smallest eigenvalues, respectively. From the left figure it is seen that the relative change in acoustic impedance for P-waves is the best-determined parameter. From the right figure it is seen that the worst-determined parameter is the relative change in P-wave velocity.

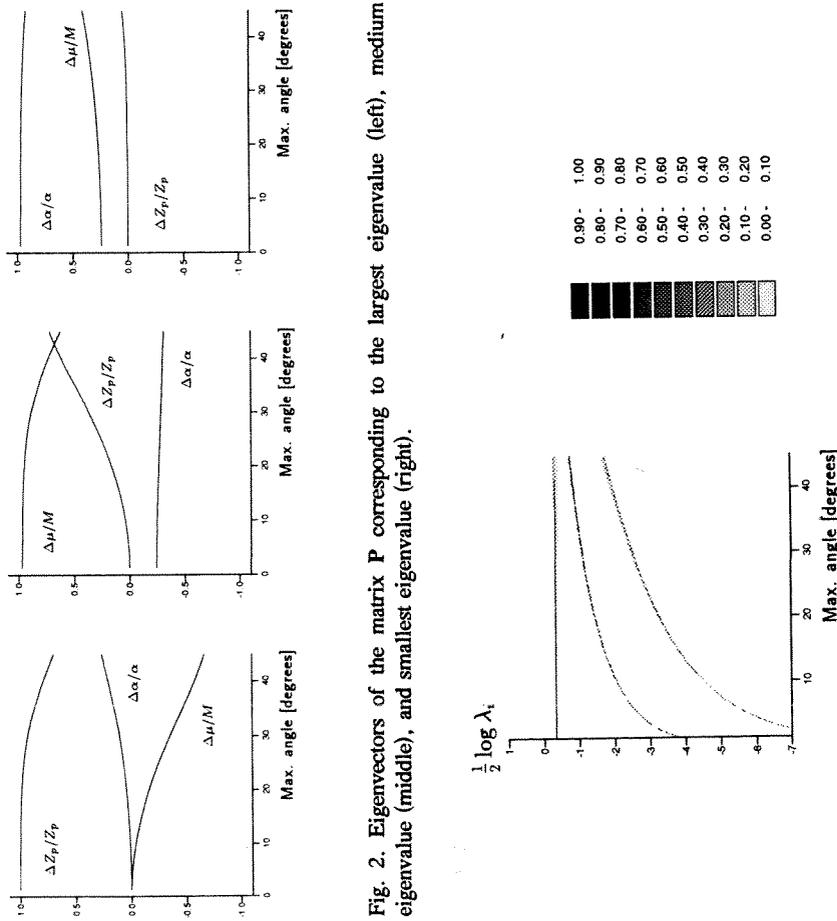


Fig. 2. Eigenvalues of the matrix **P** corresponding to the largest eigenvalue (left), medium eigenvalue (middle), and smallest eigenvalue (right).

Fig. 3. Eigenvalues of the matrix **Q**.

Fig. 3 shows the eigenvalues of the matrix **Q**. The largest and smallest eigenvalues of **Q** are about the same as the largest and smallest eigenvalues of **P**. The medium eigenvalue of **P** is, in a linear scale, 3.5, 3.3 and 2.0 times larger than the medium eigenvalue of **Q** for maximum angles of 15°, 30° and 45°, respectively. The eigenvalues are also seen to be quite insensitive to the α/β -ratio.

Fig. 4 shows the eigenvectors of the matrix **Q** arranged similarly to Fig. 2, replacing $\Delta\mu/M$ with $\Delta\nu/(1-\nu)^2$. Again the relative change in acoustic impedance for P-waves is the best-determined parameter, and the relative change in P-wave velocity the worst-determined parameter. It is seen that the eigenvectors are quite dependent on the α/β -ratio.

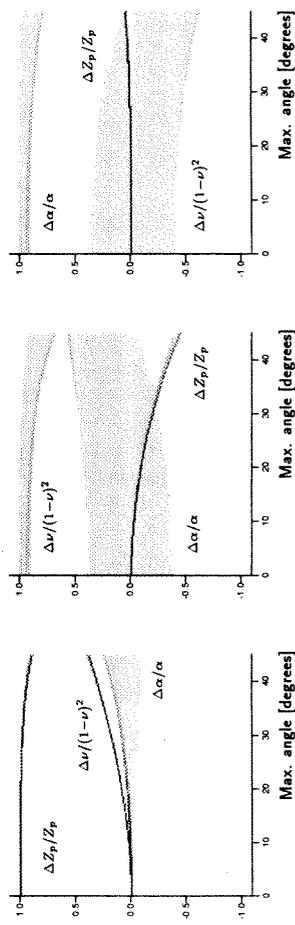


Fig. 4. Eigenvalues of the matrix **Q** corresponding to the largest eigenvalue (left), medium eigenvalue (middle), and smallest eigenvalue (right).

Fig. 5 shows the eigenvalues of the inverse normalized covariance matrix $G^{-1}RG^{-1}$ corresponding to the parameter estimate \hat{m}_1 , with $g = h = 1$ for a constant velocity layer of depth 0.5 km. The largest and medium eigenvalues are quite similar to those of **P**, whereas the smallest eigenvalue is somewhat larger.

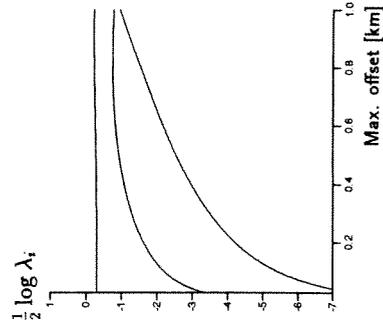


Fig. 5. Eigenvalues of the matrix $G^{-1}RG^{-1}$.

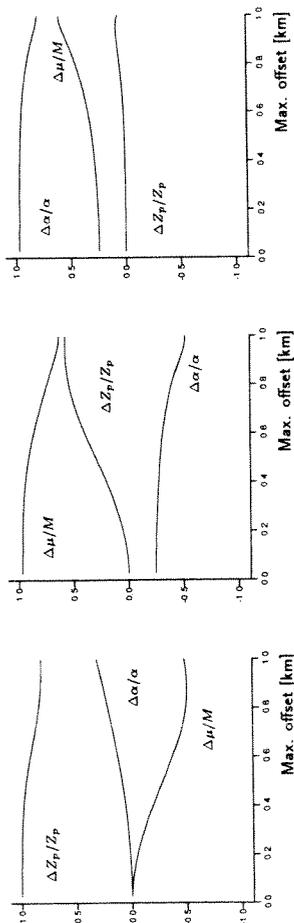


Fig. 6. Eigenvectors of the matrix $G^{-1}RG^{-1}$ corresponding to the largest eigenvalue (left), medium eigenvalue (middle), and smallest eigenvalue (right).

Fig. 6 shows components of the eigenvectors of the matrix $G^{-1}RG^{-1}$. As expected the eigenvectors are almost parallel to those seen in Fig. 2 except for large values of y_N ($y_N > 0.7$), where minor differences can be seen. Confidence regions for \hat{m} , are therefore almost parallel to the confidence regions for \hat{m}_1 except for large values of y_N or θ_k .

Fig. 7 shows the eigenvalues of the inverse normalized covariance matrix $H^{-1}RH^{-1}$ corresponding to the parameter estimate \hat{m}_2 , with $g = h = 1$ for a constant velocity layer of depth 0.5 km. The eigenvalues of the matrix $H^{-1}RH^{-1}$ are quite similar to those of the matrix Q (Fig. 3), but the smallest eigenvalue is larger.

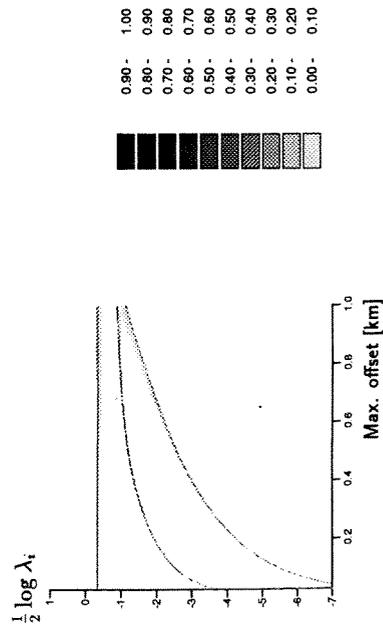


Fig. 7. Eigenvalues of the matrix $H^{-1}RH^{-1}$.

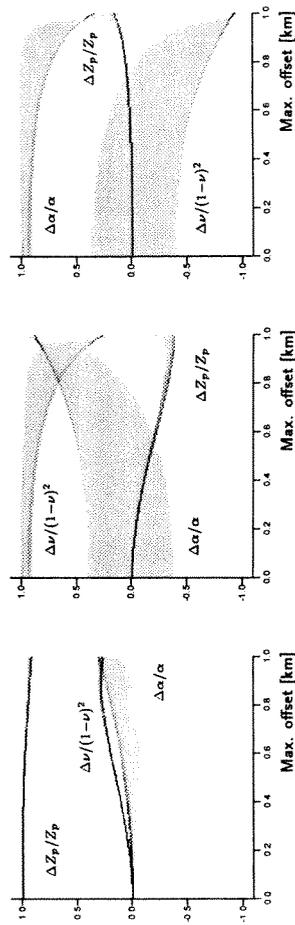


Fig. 8. Eigenvectors of the matrix $H^{-1}RH^{-1}$ corresponding to the largest eigenvalue (left), medium eigenvalue (middle), and smallest eigenvalue (right).

Fig. 8 shows components of the eigenvectors of the matrix $H^{-1}RH^{-1}$. The eigenvectors are similar to those in Fig. 4 for the matrix Q , in particular for $y_N < 0.7$ km. To clarify the plots in Fig. 8 (and Fig. 4), the eigenvectors of the matrix $H^{-1}RH^{-1}$ for a maximum offset of 0.5 km are plotted as a function of the α/β -ratio in Fig. 9. It is seen that the first eigenvector is fairly constant, while there are changes in the contribution to the second and third eigenvectors from $\Delta\alpha/\alpha$ and $\Delta\nu/(1-\nu)^2$.

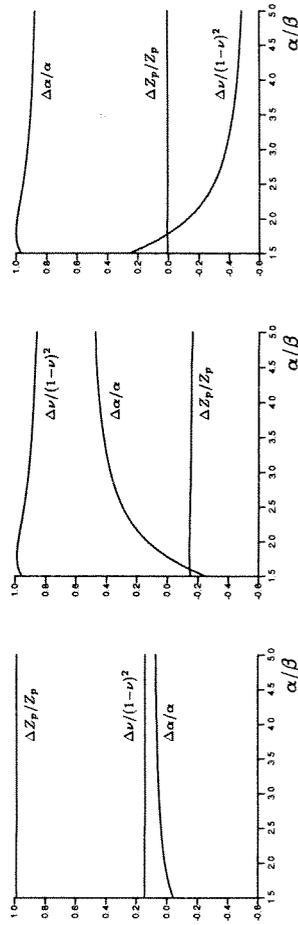


Fig. 9. Eigenvectors of the matrix $H^{-1}RH^{-1}$ corresponding to the largest eigenvalue (left), medium eigenvalue (middle), and smallest eigenvalue (right), as a function of the α/β -ratio for a maximum offset of 0.5 km.

DISCUSSION

The confidence regions above have been calculated assuming linearized PP reflection coefficients. The errors introduced by the linearization depend on the contrast in the parameters, in addition to the maximum offset. A contrast of less than 5% keeps the linearizations (1) and (3) very close to the exact Zoeppritz equations, while (5) and (11) degrade in accuracy for angles of incidence higher than about 20° (Ursin and Tjåland, 1992). Linearization will introduce bias in the modelling errors. This will cause an additional term in the covariance matrices of the estimated parameters. However, obtaining realistic estimates of error translation caused by linearization errors is, in general, difficult (Tarantola, 1987), and has not been included.

CONCLUSIONS

Different estimates of the relative change in elastic parameters have been analyzed, assuming seismic amplitude data as a function of angle or offset. Confidence ellipsoids of the different parameter estimates were studied using eigenvalue analysis. In all cases the relative change in the acoustic impedance for P-waves is the best-determined parameter. The second-best determined parameter is the change in shear modulus over the plane-wave modulus, or the normalized contrast in Poisson's ratio, depending on the parameterization. The worst-determined parameter is the relative change in P-wave velocity. The standard deviation of this parameter combination is about 3 orders of magnitude larger than that of the best-determined parameter. It therefore seems to be difficult to estimate more than two parameters from the linearized PP-reflection coefficient. The results above are in accordance with the conclusions drawn by de Nicolao et al. (1993).

The normalized change in the shear modulus is better determined than the normalized change in the Poisson's ratio. The parameterization using shear modulus therefore seems to give better results than using Poisson's ratio. From the figures it appears that for small angles, the use of offset data gives better parameter estimates than from angle data.

REFERENCES

- Aki, K. and Richards, P.G., 1980. Quantitative seismology; Theory and methods, Vol. 1. W.H. Freeman & Co, New York.
- Allen, J.L., Peddy, P.C. and Fasnacht, T.L., 1993. Some AVO failures and what (we think) we have learned. *The Leading Edge*, 12: 162-167.
- Balogh, D., Snyder, G. and Barney, W., 1986. Examples of a new approach to offset amplitude analysis. 56th Ann. Internat. SEG Mtg., Houston, Expanded Abstr.: 350-351.
- Denham, L.R., Palmeira, R.A.R. and Farrell, R. C. 1985. The zero-offset stack. 55th Ann. Internat. SEG Mtg., Washington D.C., Expanded Abstr.: 624-625.

PARAMETER ACCURACY

- de Nicolao, A., Drufuca, G. and Rocca, F., 1993. Eigenvalues and eigenvectors of linearized elastic inversion. *Geophysics*, 58: 670-679.
- Shuey, R.T., 1985. A simplification of the Zoeppritz equations. *Geophysics*, 50: 609-614.
- Smith, G.C. and Gidlow, P.M., 1987. Weighted stacking for rock property estimation and detection of gas. *Geophys. Prosp.*, 35: 993-1014.
- Swan, H.W., 1990. Noise sensitivity of linear seismic inversion. 60th Ann. Internat. SEG Mtg., San Francisco, Expanded Abstr.: 1177-1180.
- Taner, M.T. and Koehler, F., 1969. Velocity spectra - digital computer derivation and application of velocity functions. *Geophysics*, 34: 859-881.
- Tarantola, A., 1987. *Inverse Problem Theory*. Elsevier Science Publishers, Amsterdam.
- Thomsen, L., 1990. Poisson was not a geophysicist! *The Leading Edge*, 9 (12): 27-29.
- Ursin, B. and Dahl, T., 1990. Least-squares estimation of reflectivity polynomials. 60th Ann. Internat. SEG Mtg., San Francisco, Expanded Abstr.: 1069-1071.
- Ursin, B. and Dahl, T., 1992. Seismic reflection amplitudes. *Geophys. Prosp.*, 40: 483-512.
- Ursin, B. and Ekren, B.O., 1992. Robust AVO analysis. 62nd Ann. Internat. SEG Mtg., New Orleans, Expanded Abstr.: 839-843.
- Ursin, B. and Tjåland, E., 1992. Seismic amplitude analysis. 2nd SEGJ/SEG Internat. Symp. on Geotomography, Proceedings: 41-56.